Fast manometric method for determining the effective oxygen diffusion coefficient through wine stopper

Julie Chanut [1,2], Aurélie Lagorce[1,2], Sonia Lequin[1,2], Régis D. Gougeon [1,3], Jean-Marc Simon [2], Jean-Pierre Bellat [2], Thomas Karbowiak [1,*]

[1] Univ. Bourgogne Franche-Comté, AgroSup Dijon, PAM UMR 02 102, 1 Esplanade Erasme, 21000 Dijon, France

[2] Univ. Bourgogne Franche-Comté, Laboratoire Interdisciplinaire Carnot de Bourgogne, UMR 6303 CNRS, 9 Avenue Alain Savary, 21078 Dijon, France

[3] Univ. Bourgogne Franche-Comté, Institut Universitaire de la Vigne et du Vin, 1 rue Claude Ladrey, 21000 Dijon, France

[*] Corresponding Author:

Prof. Thomas Karbowiak, Univ. Bourgogne Franche-Comté, AgroSup Dijon, PAM UMR 02 102, 1 Esplanade Erasme, 21000 Dijon, France, phone number: +33380772388,

e-mail: thomas.karbowiak@agrosupdijon.fr

Abstract

A fast manometric method has been designed for determining the oxygen transfer rate through cork stoppers. Thanks to this technique, it is possible to measure the effective diffusion coefficient of oxygen through a thin cork wafer in a few days, whereas months are required in the case of a full-length cork stopper. A calculation method has also been developed and validated to extrapolate the effective oxygen diffusion coefficient measured on thin wafers to a full-length stopper, based on the statistical analysis of the experimental data distribution. The question of the material heterogeneity and the representative thickness is addressed as well as the effective length of the stopper beyond which the gain in resistance to mass transfer becomes non-significant.

Keywords: Oxygen transfer rate, Cork stopper, Diffusion, Permeability, Extrapolation method

1. Introduction

The corking represents last intervention of the winemaker for the preservation of the wine. Thereafter, the evolution of wine will depend mainly on storage conditions (temperature, relative humidity, storage position, etc.)[1-6] and on the oxygen barrier properties of the stopper in relation to the wine's ability to resist to oxidation[7]. Natural Cork stopper remains predominant with more than 80% of stoppers made of natural or colmated natural cork [8]. However, a decrease in the use of natural cork can be observed particularly over the last 20 years with the emergence of alternative stoppers such as agglomerated cork, synthetic stopper or screwcaps [8-9]. In parallel, since the mid-90s, many studies have focused on the gas barrier properties of these different types of stoppers, comparing natural corks of different quality, agglomerated corks, synthetic stoppers, and screwcaps [10-12]. Although the barrier properties of food packaging are very often indicated on technical datasheets and based on well documented standards (ISO 15105, ISO2556 and ASTM D1434)[13-15], it had required specific method development in the field of wine stoppers due to their considerable thickness. Different techniques have therefore been developed to measure the oxygen permeation through stoppers [16].

A colorimetric method has been proposed, based on the color change from the oxidation-reduction reaction of indigo carmine[17-21]. The indigo carmine solution changes from yellow in the reduced state to indigo in the oxidized state. Prior to the experiment, the reduced indigo carmine solution is introduced into a transparent wine bottle and sealed with a stopper under a continuous flow of nitrogen. The ingress of oxygen through the stopper can then be determined by colorimetric measurements of the indigo carmine solution through the transparent glass bottle over time. This method is thus nondestructive and close to the real conditions of wine storage in bottle.

Another non-invasive method is the detection of oxygen by chemiluminescence[22-25]. This technique is based on a sensor dot containing a luminophore sensitive to oxygen. The sensor is glued inside a transparent bottle before being filled with wine. It is then used to measure the dissolved oxygen concentration as well as the oxygen headspace concentration, depending on the position of the sensor in the bottle. As with the previous method, the measurement is carried out through the glass bottle, in this case using an optical fiber. The luminescence decay time is correlated with the oxygen concentration inside the bottle.

Coulometric method consists in measuring the oxygen flow going through a cork stopper inserted in a bottleneck when a constant oxygen pressure is applied to one side of the stopper while the other side is flushed with nitrogen. The oxygen passing through the stopper is then detected by a coulometric detector composed of a silver cathode and a lead anode. Unlike the two previous methods, the measurement is carried out at 0% relative humidity using an oxygen pressure gradient of 1013 hPa or 212 hPa, the latter corresponding to the oxygen partial pressure in the atmosphere while the former is equivalent to the atmosphere pressure. This method is based on ASTM standard F1927, which defines a procedure for "the determination of the rate of transmission of oxygen gas through film, sheeting, laminates, co-extrusions, or plastic-coated papers or fabrics"[26].

Oxygen transfer through wine stoppers can also be estimated by titrating the SO_2 present in the wine. This is an indirect method, which is based on the assumption that the loss of SO_2 in the wine over time is proportional to the consumption of oxygen brought into the bottle through the stopper. The most commonly used methods are the Rankine and Pocock[27] and the Ripper methods[28]. However, the oxygen transfer rate can be overestimated because the loss of SO_2 in the wine over time is not only due to its reaction with oxygen.

Lastly, the manometric method can be used to determine the oxygen transfer through wine stoppers. This technique is based on measuring the pressure in two closed compartments separated by the stopper[29-30]. Prior to experiment, the sample is usually outgassed under vacuum in order to remove volatile compounds from the stopper. Oxygen is introduced into the first compartment, at 212 hPa or 1013 hPa. The second compartment is then placed either in a dynamic or static vacuum. In the former case, the oxygen transfer through the sample is monitored by the pressure decrease in the first compartment over time. In the latter case, the transfer is followed by the pressure increase in the second compartment over time. In both cases, the oxygen transfer is calculated based on Fick's law applied to the steady state. In order to reduce experimentation time, the full-length stopper can be replaced by a thin wafer and the second compartment maintained under dynamic vacuum [31-36]. In that case, the experimental results obtained on a thin wafer can then be extrapolated to a full-length stopper provided that enough replicates are carried out to obtain a statistically fair distribution. Unlike previous methods which are dedicated only to oxygen transfer, this method can be used for any other gas and over a wide range of pressures. It has recently been applied to study the CO_2 barrier properties of sparkling wine stoppers at a higher-pressure difference (0.6 MPa). However, this method is often used at 0 % relative humidity on dry samples and may derivate from real conditions.

In this article, we present the versatility of the manometric method used here to study the transfer of oxygen through two different types of wine stoppers: natural cork and agglomerated cork. First, permeation experiments were performed on the thinnest possible wafers in order to quickly determine the effective diffusion coefficients of oxygen through these samples. Then, a specific statistical extrapolation method has been developed and validated with data obtained on full-length samples. Lastly, the effective diffusion coefficients of oxygen through stoppers of various lengths were calculated from these data by using this extrapolation.

2. Theory and Calculation

2.1. Sorption of oxygen

Sorption of oxygen by cork was studied by manometry with a specific apparatus built in the laboratory. The sorption isotherm was measured on cubic pieces (edge of about 3 mm) at 298 K for pressures ranging from 0.1 to 1000 hPa. Prior to sorption, cork was outgassed under dynamic primary vacuum (0.1 hPa) for 2 days to remove gases and vapors (essentially water) sorbed at room temperature during the previous storage. The sorption isotherm was then measured step by step by applying successive pressures of oxygen in contact with the sample. When the sample is exposed to oxygen, the pressure decreases, due to the sorption of oxygen by cork. Once equilibrium is reached, the amount of oxygen sorbed is determined by performing a mass balance in the gas phase from the pressure measured before and after each sorption step.

2.2. Oxygen permeation

2.2.1. Experimental procedure

The oxygen transfer through cork samples was investigated using a homemade apparatus based on a manometric method (Figure 1)[33, 35]. This technique allowed the measurement of the oxygen flow passing through a cork wafer, or a full-length cork sample, stuck into a metal ring seal separating the two chambers C_1 and C_2. First, an oxygen purge was performed in the measuring chamber C_1. An initial pressure of 900 hPa of oxygen was then introduced while the other compartment, C_2, was kept under dynamic vacuum (0.1 hPa). The decrease in oxygen pressure in the measuring compartment, caused by the transfer of oxygen from compartment C_1 to compartment C_2, was recorded over time. The temperature was kept constant at 293 (± 1) K by a thermostatically controlled water circulation surrounding compartment C_1. The pressure sensitivity was ± 0.1 hPa.

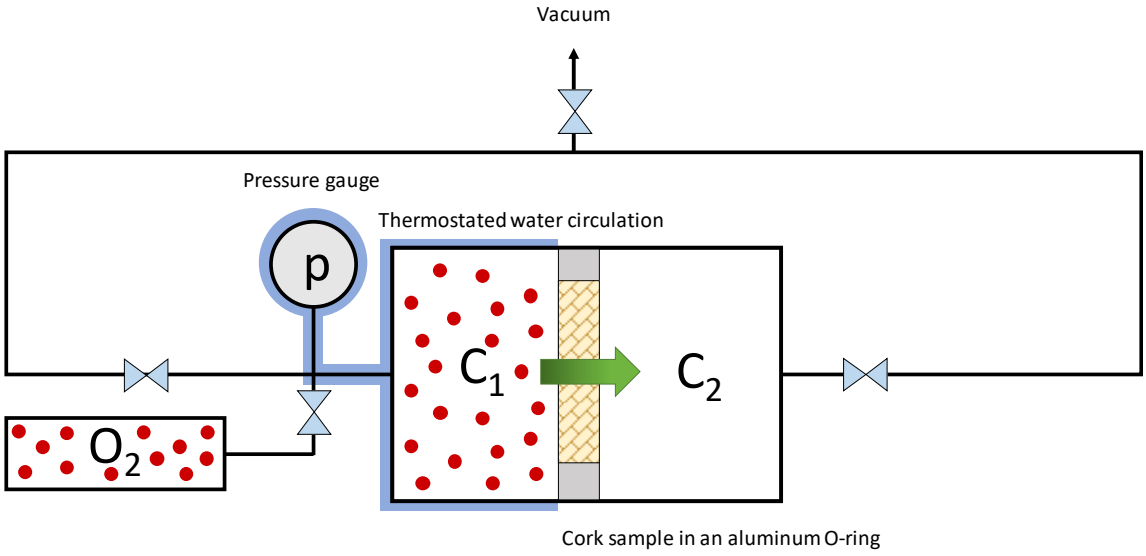

Figure 1: Scheme of the home-made manometric device used to measure oxygen transfer through wine stoppers.

2.2.2. Analysis of oxygen transfer in cork stopper

The phenomenon of permeation is classically described as a three-steps mechanism: (i) firstly, sorption of gas molecules on the surface of the material. (ii) Secondly, diffusion through the material according to the concentration gradient; (iii) lastly, instantaneous desorption from the other surface of the material. The corresponding profile of concentration along the direction perpendicular to the cork wafer is shown in Figure 2.

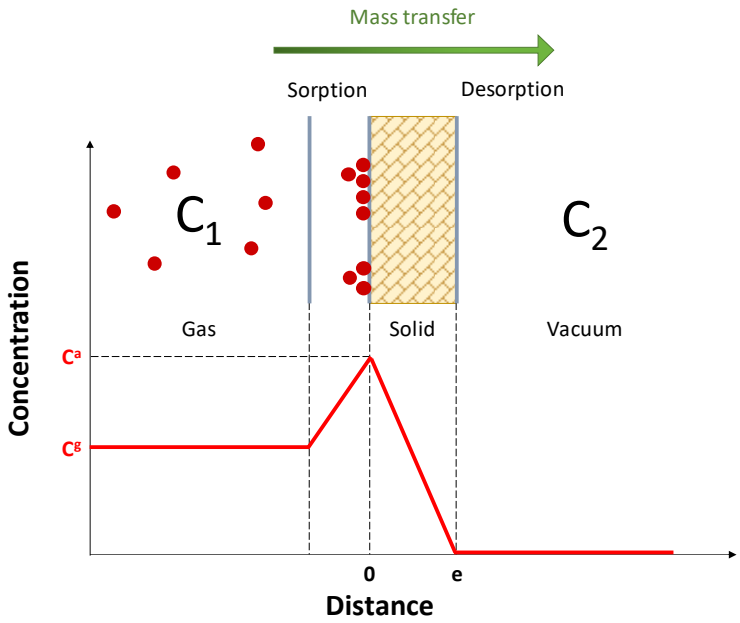

Figure 2: Profile of gas and sorbate(oxygen) concentrations along the direction perpendicular to the solid sample (cork wafer).

Considering the gas as ideal, the surface molar flow of oxygen passing through the wafer, J_w (mol.m^{-2}.s^{-1}), is given by the equation:

$$J_w = -\frac{1}{S_w}\frac{dN}{dt} = -\frac{V}{S_w.R.T}\frac{dp}{dt} \qquad \text{(Equation 1)}$$

p is the pressure (Pa) in the compartment C_1 along time t (s), V is the volume of the compartment C_1 (m^3), S_w is the surface of the wafer (m^2), R is the ideal gas constant (8.314 J.mol^{-1}.K^{-1}), T is the temperature (K) and N is the amount of oxygen (mol).

According to the first Fick's law, the surface molar flow of oxygen passing through the cork wafer J_w, once the steady state has been established, is also given by the equation:

$$J_w = -D_w.\nabla C^a \approx -D_w.\frac{C^a}{l_w} \qquad \text{(Equation 2)}$$

With D_w the diffusion coefficient (m^2.s^{-1}) of oxygen inside the wafer, l_w the thickness of the wafer (m) and ∇C^a (mol.m^{-4}) the concentration gradient of oxygen sorbed on both sides of the wafer. C^a (mol.m^{-3}) is related to the concentration of the gas C^g (mol.m^{-3}) by the equation:

$$C^a = \psi . C^g \quad \text{(Equation 3)}$$

With ψ, so called the separation factor or partitioning coefficient, which depends on the gas concentration. ψ is calculated from the sorption isotherm of oxygen.

By combining the equations (1), (2) and (3), and after integration over time, we obtain:

$$\ln\left(\frac{p_{t=0}}{p_t}\right) = \frac{D_w.\psi.S_w}{l_w.V}.t \quad \text{(Equation 4)}$$

Thus, the diffusion coefficient of oxygen through the cork wafer is determined from the linear regression of $\ln\left(\frac{p_{t=0}}{p_t}\right) = f(t)$ obtained once the steady state is reached.

2.2.3. Extrapolation of the oxygen diffusion coefficient from a thin wafer to a full-length stopper

As the cork stopper is not a homogeneous material, the diffusion coefficient measured through a thin cork wafer of thickness l_w is not representative of the diffusion coefficient through a full-length cork stopper of length l_s. Indeed, the concentration of defects (as lenticels) depends on the region where the wafer has been cut in the stopper. From the measurements made on thin wafers, it is thus necessary to extrapolate the experimental results to a full-length cork stopper. To that end, the stopper can be considered as a stack of n wafers in series where each slice represents a local resistance to gas transfer, R_w as illustrated in Figure 3. Resistance is an extensive property that increases with size sample. In our case, the resistance to mass transfer of each wafer is defined by the ratio $R_w = \frac{l_w}{D_w}$. By analogy with an electric circuit, the overall resistance to mass transfer of the whole stopper is the sum of the individual resistances of the wafers into which the stopper can be decomposed.

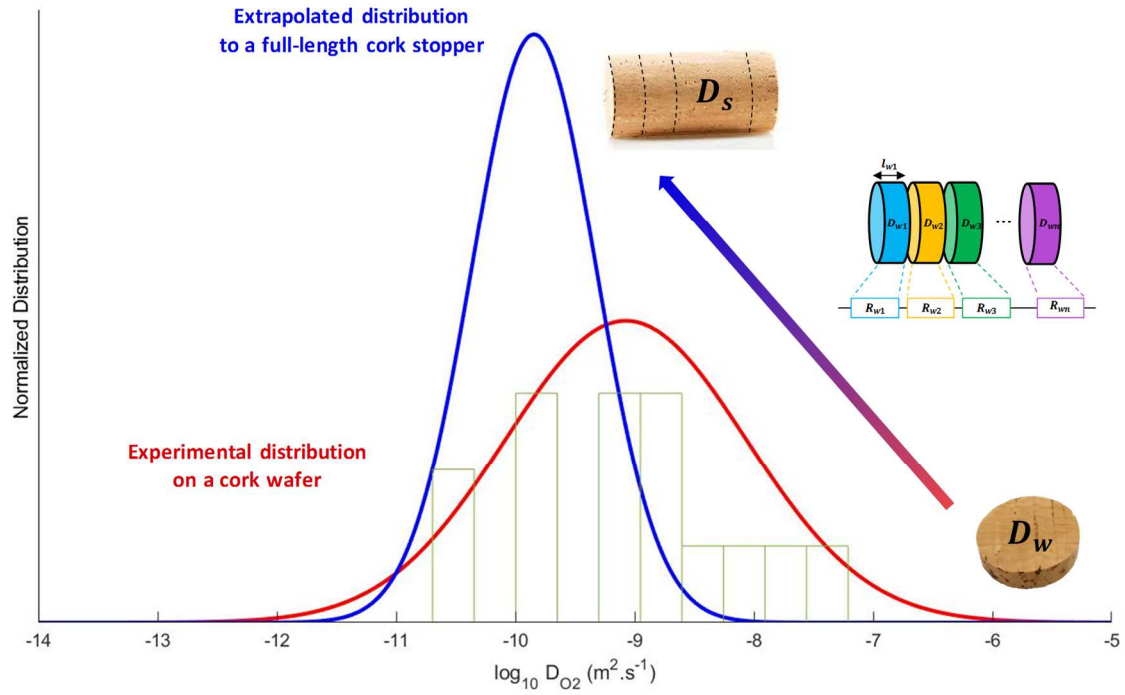

Figure 3: Experimental data (□ green rectangle) of the logarithm of the effective oxygen diffusion coefficient measured on cork wafers, corresponding experimental distribution (- red line), and extrapolated distribution (- blue line) of the logarithm of the effective oxygen diffusion coefficient of a full-length cork stopper, at 298 K.

The sum of these resistances was used to calculate the total resistance of the stopper R_s, according to the following equations:

$$R_s = \frac{l_s}{D_s} = \sum_{i=1}^{n} R_{wi} = \sum_{i=1}^{n} \frac{l_{wi}}{D_{wi}} \quad \text{(Equation 5)}$$

$$l_s = l_w . n \quad \text{(Equation 6)}$$

$$\frac{1}{D_s} = \frac{1}{n} \sum_{i=1}^{n} \frac{1}{D_{wi}} \quad \text{(Equation 7)}$$

With R_s the overall resistance of the stopper, D_s the extrapolated diffusion coefficient in the stopper, l_s the total length of the stopper, n the total number of wafers composing in a full-length stopper and D_{wi} the diffusion coefficient of the wafer i drawn at random in the statistical distribution of diffusion coefficients determined experimentally.
This model can be applied to determine the extrapolated diffusion coefficient in stoppers having different lengths, from 3 mm which is the minimum cork thickness required for oxygen transfer measurement up to 54 mm, the maximum length of stopper used for still wine. As an example, considering a 48 mm length cork stopper, 16 diffusion coefficient values are randomly taken from the statistical distribution of 3 mm cork wafers to calculate the mean diffusion coefficient through a 48 mm cork stopper. In order to obtain a fair statistical distribution of oxygen diffusion coefficients through the whole cork stopper, this procedure is repeated 10^4 times. For this purpose, a specific code has been developed on the Matlab software.

It is worthy to note that equation 7 is a simplification that applies to a homogeneous material composed of successive layers of the same material (equivalent to a single phase at the macroscopic scale considered). If the stopper is composed of different phases with different diffusion coefficients and different solubilities of oxygen, its overall diffusion coefficient must be determined according to the more general Equation 8:

$$\frac{l_s}{D_s . \psi_s} = \sum_{i=1}^{n} \frac{l_i}{D_i . \psi_i} \quad \text{(Equation 8)}$$

3. Materials

3.1. Natural cork stopper

High quality (grade 0) natural cork stoppers, from *Quercus suber L.* oak tree in the Mora (Portugal) production area were used. Stoppers were neither washed nor surface treated with a coating agent prior to use. The dimensions of stoppers were 24 mm in diameter and 49 mm in length, with a mean density of 182 (± 20) kg.m^{-3}.

3.2. Microagglomerated cork stopper

Micro-agglomerated cork stoppers “Diam 10” were produced with a molding process using cork particles (between 0.3 and 1.5 mm) associated with binding agents. The stoppers used for the

experiments had a diameter of 24.2 mm and a length of 49 mm and had not undergone any surface treatment. The samples had a mean density of 295 (± 7) kg.m^{-3}.

3.3. Sample preparation

For the natural cork stoppers, fifteen wafers were manually cut from the middle of fifteen different stoppers following the axial section. Final dimensions were 24 mm in diameter and 6 mm thick. For the microagglomerated stoppers, ten 3-mm thick cork wafers were cut in the middle of full-length stoppers.

Prior to oxygen permeation measurement, both wafers from natural and agglomerated cork, as well as full-length stoppers, were inserted without compression into a metal ring and glued at the periphery with Araldite 2011 to prevent gas transfer at the interface. Blank experiments performed with metal wafer stuck into the metal ring instead of the cork wafer showed that no diffusion through glue film is observed.

4. Results and Discussion

4.1. Sorption of oxygen on cork

The sorption isotherm of oxygen on cork powder at 298 K is displayed in Figure 4. It exhibits a type III shape according to the IUPAC classification[37]. It is characteristic of the adsorption on a nonporous or microporous material with a weak adsorption affinity.

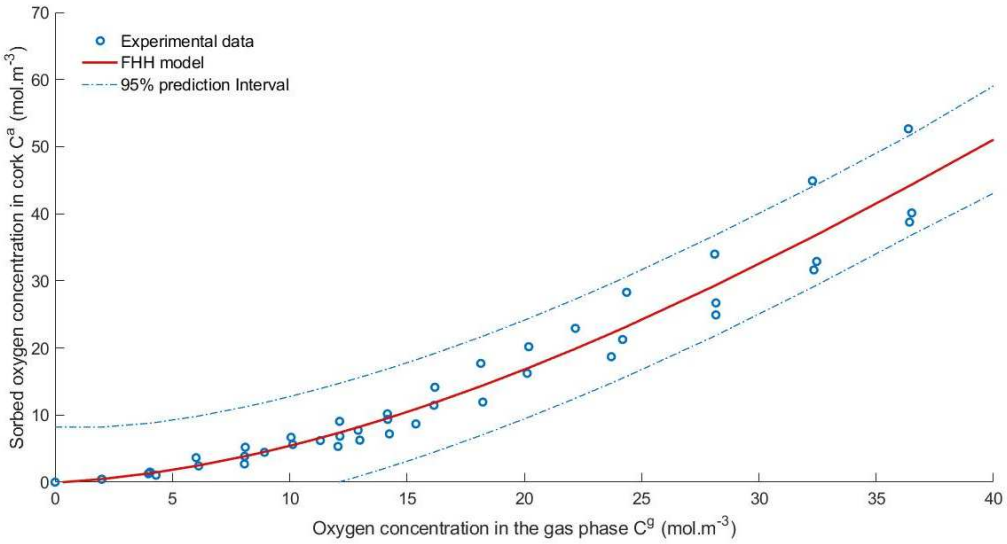

Figure 4: Sorption isotherm of oxygen on cork at 298 K for oxygen pressure ranging between 0 and 1000 hPa (o experimental data, - FHH model used to fit sorption data, -.- 95% prediction interval); (data from Lequin et al.[33])

The sorption isotherm is well fitted with the Frenkel, Halsey and Hills (FHH) model, as defined by the following relationship (Eq. 9)

$$\frac{C^a}{C_m} = [K_{FHH.} \ln\left(\frac{C_s^g}{C^g}\right)]^{-1/s} \qquad \text{(Equation 9)}$$

Where C^g is the concentration of oxygen in the gas phase, C^a is the concentration of sorbed oxygen in the cork, C_m is the concentration of sorbate in the "equivalent" monolayer (first layer of oxygen molecules sorbed on the surface), C_s^g is the concentration of gas in equilibrium with its liquid phase

at the sorption temperature, K_{FHH} is an adjustable parameter related to the energy of sorption, and s is related to the nature of gas−solid interaction.

First, the oxygen saturation vapor pressure p_s was determined using Antoine's equation (Eq. 10) in order to calculate C_s^g.

$$\log_{10}(p) = A - \frac{B}{T+C} \quad \text{(Equation 10)}$$

With Antoine's coefficients A, B and C (A=3.9523, B=340.024 and C =-4.144 in the case of oxygen[38]), p is the pressure (bar) and T is the temperature (K). These coefficients were determined for a temperature range between 54 and 154 K. Nevertheless, they are used here to estimate p_s the saturation vapor pressure of oxygen by extrapolating to 298 K. The concentration C_s^g, calculated by the relation $C_s^g = \frac{p_s}{R.T}$, is equal to 25 186 mol.m^{-3}.

Once C_s^g was known, the adjustable parameters of the FHH model were determined, using a code developed on the Matlab software. The parameters are shown in Table 1 and the corresponding modeling in Figure 4. The coefficients obtained are similar to those previously determined by Lagorce *et al*.[35].

Table 1 : Parameters of the FHH model for oxygen sorption by cork at 298K.

C_m (mol.m^{-3})	K_{FHH}	C_s^g (mol.m^{-3})	s
7.8832	0.1318	25 186	0.0883

This model allows to accurately calculate the value of ψ, which is required to determine the diffusion coefficient (Eq. 4). Using extrapolation by modeling, it can even be used to estimate ψ for measurements performed at a higher initial oxygen pressure.

4.2. Effect of the initial pressure of oxygen on the effective diffusion coefficient

Oxygen permeability measurements were carried out on agglomerated cork wafers using different initial pressures ranging from 1 x 10^3 to 4 x 10^3 hPa. The ψ value used to calculate the oxygen diffusion coefficient was determined using the model detailed in previous section. Figure 5 displays, the log ratio of the effective diffusion coefficient measured at initial oxygen pressure of 1 x 10^3, 2 x 10^3, 3 x 10^3 and 4 x 10^3 hPa to the value measured at 1 x 10^3 hPa. For this specific experiment, 6 mm thick wafers were used, as 3 mm thick wafers broke due to a too high pressure gradient between the two compartments when reaching 4 x 10^3 hPa.

It is noteworthy that the value of the effective diffusion coefficient remains similar whatever the initial oxygen pressure (Fig. 5). All values obtained at 2 x 10^3 hPa, 3 x 10^3 hPa and 4 x 10^3 hPa are not significantly different from the effective oxygen diffusion coefficient measured at 1 x 10^3 hPa. In this pressure range, the diffusion coefficient therefore appears to be independent of the initial oxygen pressure.

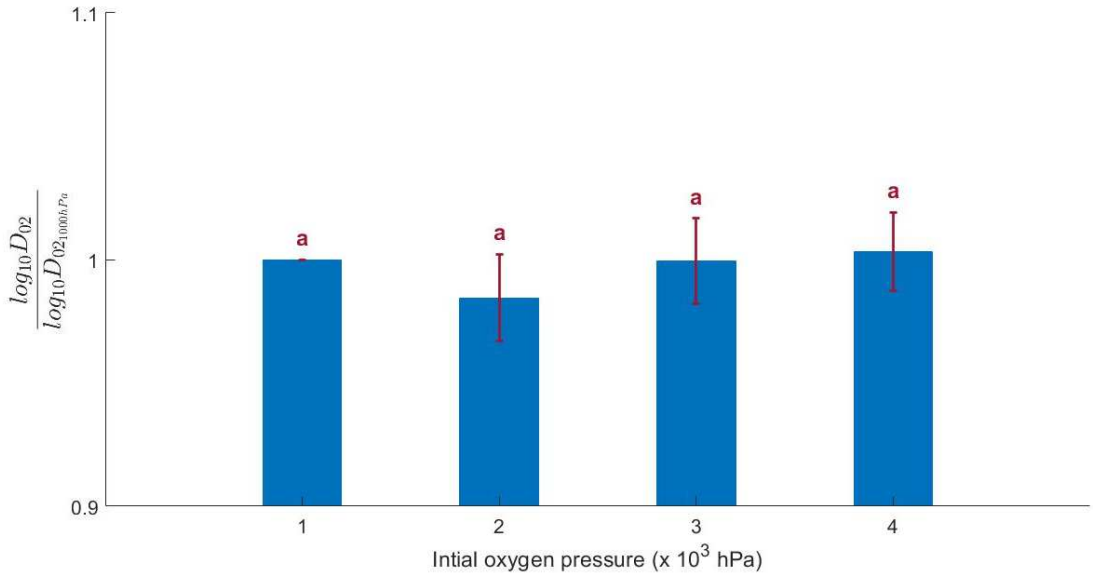

Figure 5: Log ratio of the effective diffusion coefficient measured at initial oxygen pressure increasing to the value at 1000 hPa (n=5). The superscript letter refers to the ANOVA test with a p-value of 0.05.

4.3. Validation of the extrapolation model from a wafer to a full-length stopper

In order to validate the extrapolation model, oxygen permeability measurements were carried out on full-length cork stoppers (for both natural and agglomerated stoppers). The values obtained were then compared with those extrapolated from the permeability measurements carried out on cork wafers. Figure 6 shows the distribution of effective oxygen diffusion coefficients measured on full-length stoppers and the extrapolated distribution both for natural and agglomerated corks. In the case of the natural cork stopper, fifteen repetitions were performed on the 6-mm thick cork wafer and fifteen on full-length cork stopper. In the case of agglomerated cork stopper, ten 3-mm thick wafers and ten full-length cork stoppers were used. For thin wafers, an initial oxygen pressure of 900 hPa was used. As D_{O_2} does not depend on the initial pressure (Fig. 5), measurements on full-length stoppers were performed using an initial pressure of 4 x 10^3 hPa in order to reduce the time of experimentation.

The values of effective oxygen diffusion coefficient through 6 mm natural cork wafers (Figure 6A, green dash-dotted line) spread over 5 decades, with values ranging from 10^{-6} to 10^{-12} $m^2.s^{-1}$, and a maximum at 84 x 10^{-11} $m^2.s^{-1}$. From these experimental data, the effective oxygen diffusion coefficient through a 48 mm length cork stopper is extrapolated according to the model detailed in the material and method section and exemplified in Figure 3. The calculation takes into account the statistical distribution of the experimental data. In this case, the value of effective oxygen diffusion coefficient is 14 x 10^{-11} $m^2.s^{-1}$ and the width of the distribution is reduced to three decades (Figure 6A, green line). In the case of full-length cork stoppers with a thickness of 49 mm, the values of effective oxygen diffusion coefficient are distributed between 10^{-6} $m^2.s^{-1}$ to 10^{-13} $m^2.s^{-1}$ with a maximum at 19 x 10^{-11} $m^2.s^{-1}$ (Figure 6A, blue dash-dotted line).

For agglomerated cork stopper samples, the values of effective oxygen diffusion coefficient through 3 mm wafers lie between 10^{-12} and 10^{-10} $m^2.s^{-1}$, with a maximum at 1.7 x 10^{-11} $m^2.s^{-1}$ (Figure 6B, green dash-dotted line). When extrapolated to a 48 mm stopper, the effective diffusion coefficient gives a

value of 1.4 x 10^{-11} $m^2.s^{-1}$. Lastly, for a full-length stopper, the experimental distribution is about 10^{-11} $m^2.s^{-1}$ with a maximum at 1.8 x 10^{-11} (Figure 6B, blue dash-dotted line).

For both types of stoppers, in the case of the full-length stopper, the extrapolated distribution of the effective oxygen diffusion coefficient is thus superimposed on the experimental distribution of the effective oxygen diffusion coefficient. The extrapolation model is therefore reliable for determining the diffusion coefficient of a cork stopper from values measured on a thin wafer. This extrapolation method can be generalized in its application to all other types of stoppers. In each case, it is important to carefully choose the minimum thickness of the sample which provides the best balance between a short experimental time with a good representativeness of the heterogeneity of the material.

A) Natural Cork

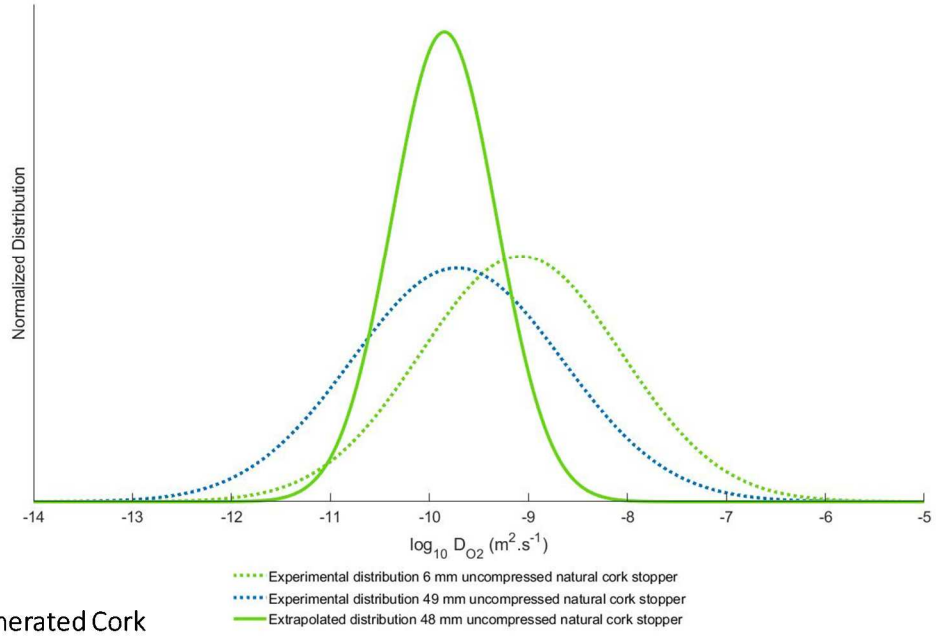

B) Agglomerated Cork

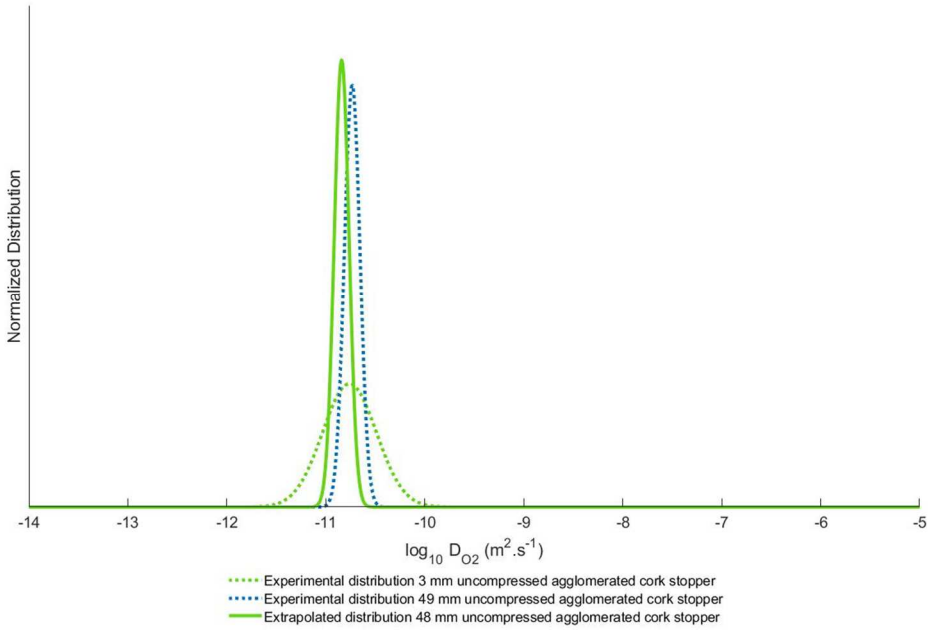

Figure 6 : Experimental distribution of effective oxygen diffusion coefficients measured on thin wafers of 3 mm or 6 mm thickness (--- green dash-dotted line), extrapolated distribution of the logarithm of the effective oxygen diffusion coefficient for a 48 mm length stopper, (- green line) and effective diffusion coefficient of oxygen for a 49 mm full-length stopper (-- blue dash-dotted line). A) Case of Natural cork (n=15), B) Case of Agglomerated cork (n=10).

4.4. *Effect of the heterogeneity of the material*

The distribution of effective oxygen diffusion coefficients measured on wafers and extrapolated to a full-length stopper, both for natural and agglomerated corks, are given in Figure 7 and in Table 2. The harmonic and arithmetic means are also reported. The harmonic mean is defined as the reciprocal of the arithmetic mean of the reciprocals. It is used when there is inverse proportionality relationship, such as between the resistance and the reciprocals of the diffusion coefficient. Indeed, the resistance of the wafer to mass transfer is defined by the ratio $R_w = \frac{l_w}{D_w}$.

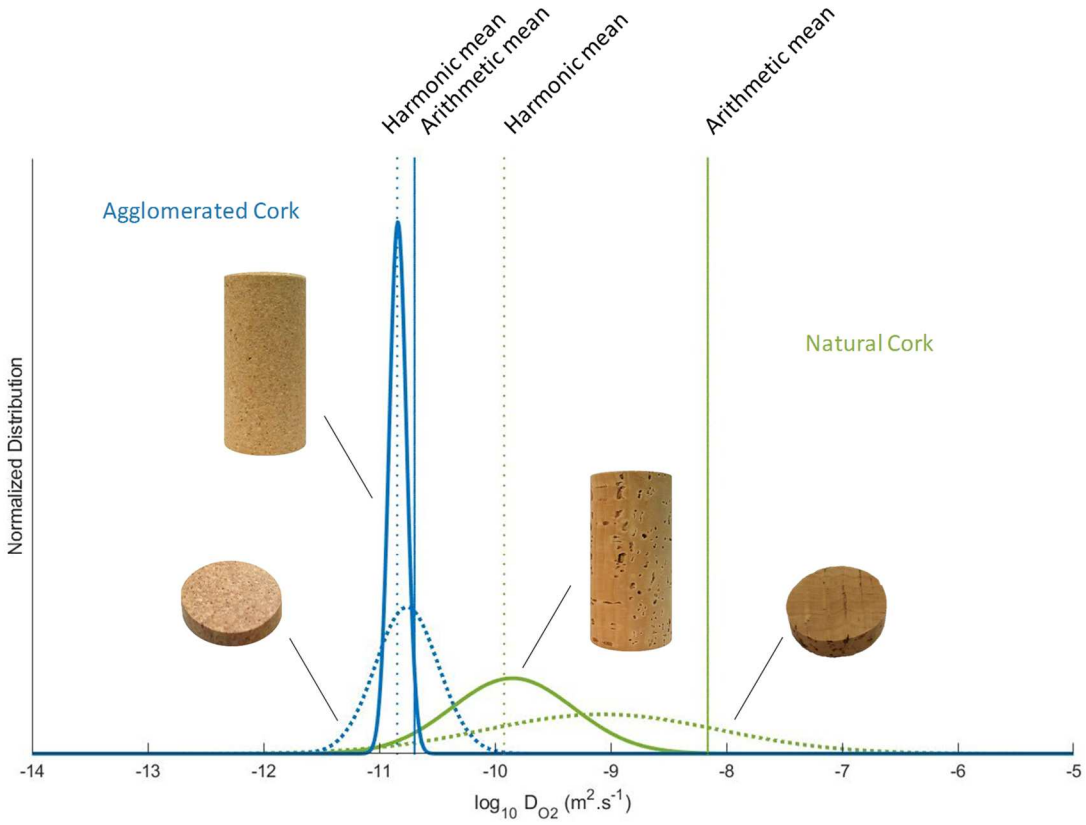

Figure 7: Experimental distribution of the logarithm of the effective oxygen diffusion coefficient measured on a 3 mm wafer for an agglomerated stopper and on 6 mm for a natural cork stopper, at 298 K (dash-dotted line). Extrapolated distribution of the logarithm of the effective oxygen diffusion coefficient for a 48 mm length stopper, at 298 K (solid line). The mean value, obtained from the harmonic mean of the experimental data, is indicated by a vertical dotted line. The mean value, obtained from the arithmetic mean, is indicated by a vertical solid line. Case of the natural cork stopper (in green). Case of the agglomerated cork stopper (in blue).

The arithmetic and harmonic means, calculated from the values of the effective oxygen diffusion coefficient through 6 mm natural cork wafers are of 691 × 10^{-11} $m^2.s^{-1}$ and 12 x 10^{-11} $m^2.s^{-1}$, respectively. As detailed in the previous section, when extrapolated to a full-length cork stopper, the peak value of effective oxygen diffusion coefficient is 14 x 10^{-11} $m^2.s^{-1}$. Such a difference between the extrapolated effective diffusion coefficient value and the arithmetic mean value (more than one

order of magnitude higher) highlights the fact that the effective diffusion coefficient for the whole cork stopper cannot be simply calculated as the arithmetic mean. Indeed, due to the heterogeneous nature of cork, each single measurement made on 6 mm wafers is not directly representative of the diffusion coefficient in a full stopper.
The transfer of oxygen through cork is not the same in the different parts of the material (i.e. the phellem and the lenticels)[39]. Consequently, this leads to differences between natural cork samples which have different ratios of lenticular channels at the 6 mm thickness scale. However, this heterogeneity is taken into account when using the extrapolation based on the statistical distribution. For this reason, a high number of replications must be performed.

When considering agglomerated cork stopper samples, the arithmetic and harmonic means of the effective diffusion coefficient show fairly similar values of 2.0 x 10^{-11} $m^2.s^{-1}$ and 1.4 x 10^{-11} $m^2.s^{-1}$, respectively. Extrapolated to a full-length stopper, the effective diffusion coefficient gives a value of 1.4 x 10^{-11} $m^2.s^{-1}$. Therefore, agglomerated cork appears to be a more homogeneous system than natural cork, as similar values are obtained for the extrapolated value and the arithmetic mean. Indeed, this material is composed of a mixture of cork particles of small size (≤ 1 mm in diameter) which are trapped in an adhesive network consisting of polyurethane binder. As the cork particles have no specific orientation in this case, this also confers on the macroscopic scale a greater isotropy to the agglomerated stopper compared to the natural cork stopper.

Table 1: Effective diffusion coefficient of oxygen and corresponding oxygen transmission rate (OTR) in natural and agglomerated cork stoppers, determined by different methods. (n=15 for Natural cork and n=10 for agglomerated cork). OTR was calculated for a stopper with a length of 49 mm and a diameter of 18.5 mm with an oxygen pressure differential of 200 hPa. It is given in mg.year-1, referring to as mg of oxygen going through the stopper per year. Data in brackets are minimum and maximum values including standard deviation from the corresponding distribution (Fig. 6 and Fig.7).

	Natural Cork		*Agglomerated Cork*	
	D_{O2} (x 10^{-11} $m^2.s^{-1}$)	OTR (mg.year^{-1})	D_{O2} (x 10^{-11} $m^2.s^{-1}$)	OTR (mg.year^{-1})
Gaussian model applied to experimental data obtained on thin cork wafers (6 mm for natural cork and 3 mm for agglomerated cork)	84.4 *(8.2-866.6)*	7.9 *(0.8-81.3)*	1.7 *(0.9-3.2)*	0.16 *(0.09-0.30)*
Arithmetic mean of the experimental data on cork wafers	691	64.8	2.0	0.19
Harmonic mean of the experimental data on cork wafers	12.0	1.1	1.4	0.13
Extrapolation to a 48 mm length stopper from the statistical distribution of the experimental data	14.4 *(4.2-48.8)*	1.3 *(0.4-4.6)*	1.4 *(1.2-1.7)*	0.14 *(0.11-0.16)*
Experimental distribution on 49 mm length stopper	19.0 *(1.6-220.4)*	1.8 *(0.15-20.6)*	1.8 *(1.5-2.2)*	0.17 *(0.14-0.21)*

In addition, the calculation of the harmonic mean provides values close to those obtained by the statistical method. This gives values of 12 x 10^{-11} $m^2.s^{-1}$ for natural cork and 1.4 x 10^{-11} $m^2.s^{-1}$ for agglomerated cork, respectively. The harmonic mean can thus be used, as a first approximation, to determine the effective diffusion coefficient, before further use of the proposed statistical method, which requires the development of a specific code on software such as Fortran or Matlab.

4.5. Extrapolation to different lengths of stopper

The nature of the cork can affect the consumer's perception of the quality of the wine. A natural cork stopper is perceived favorably by the consumer compared to a synthetic stopper or a screw cap, and may even convey this perception to the quality of the wine[40]. Cork-based stoppers are available on the market in different lengths, typically from 38 mm up to 54 mm. Length can also have an impact on the perception of the quality of the wine by the consumer, assuming that the longer the stopper, the less the oxygen enters in the bottle and thus the better the wine will age. The use of the extrapolation method we proposed could be helpful to address the question of the influence of the stopper length on the oxygen transfer. In this study, the effective length is defined as the length above which the decrease in the diffusion coefficient becomes insignificant. To determine such effective length, the ratio of the oxygen diffusion coefficient in the stopper at the length i to the oxygen diffusion coefficient in the stopper at the length $i-1$, is calculated as shown in equation 8. When the ratio vanishes below 10%, we considered that there is no significant change in the oxygen diffusion coefficient. This ratio was arbitrarily chosen, considering a 10% gain in the diffusion coefficient as insignificant compared to the standard deviations usually obtained on the values of diffusion coefficient.

$$100 - \frac{D_i}{D_{i-1}}.100 < 10\ \% \qquad \text{(Equation 8)}$$

Successive extrapolations of the effective oxygen diffusion coefficients were made from the experimental distribution of the wafers, both varying the length of the stopper from 6 to 54 mm. The influence of the stopper length on the effective oxygen diffusion coefficient is shown in Figure 8A and 8B, for natural and agglomerated corks stoppers, respectively.

In the case of natural cork (Figure 8A), when the length of the stopper increases, the corresponding distribution of D is reduced with values which lie between 10^{-9} for 6 mm length and 10^{-10} $m^2.s^{-1}$ for the maximum length of 54 mm. Moreover, above 36 mm, there is no longer significant decrease (≤ 10 %) in the effective oxygen diffusion coefficient, which tends towards the value of 1.4 x 10^{-10} $m^2.s^{-1}$. When similar successive extrapolations are applied in the case of the agglomerated stopper (Figure 8B), the effective length is 6 mm, with an effective oxygen diffusion coefficient of 1.4 x 10^{-11} $m^2.s^{-1}$.

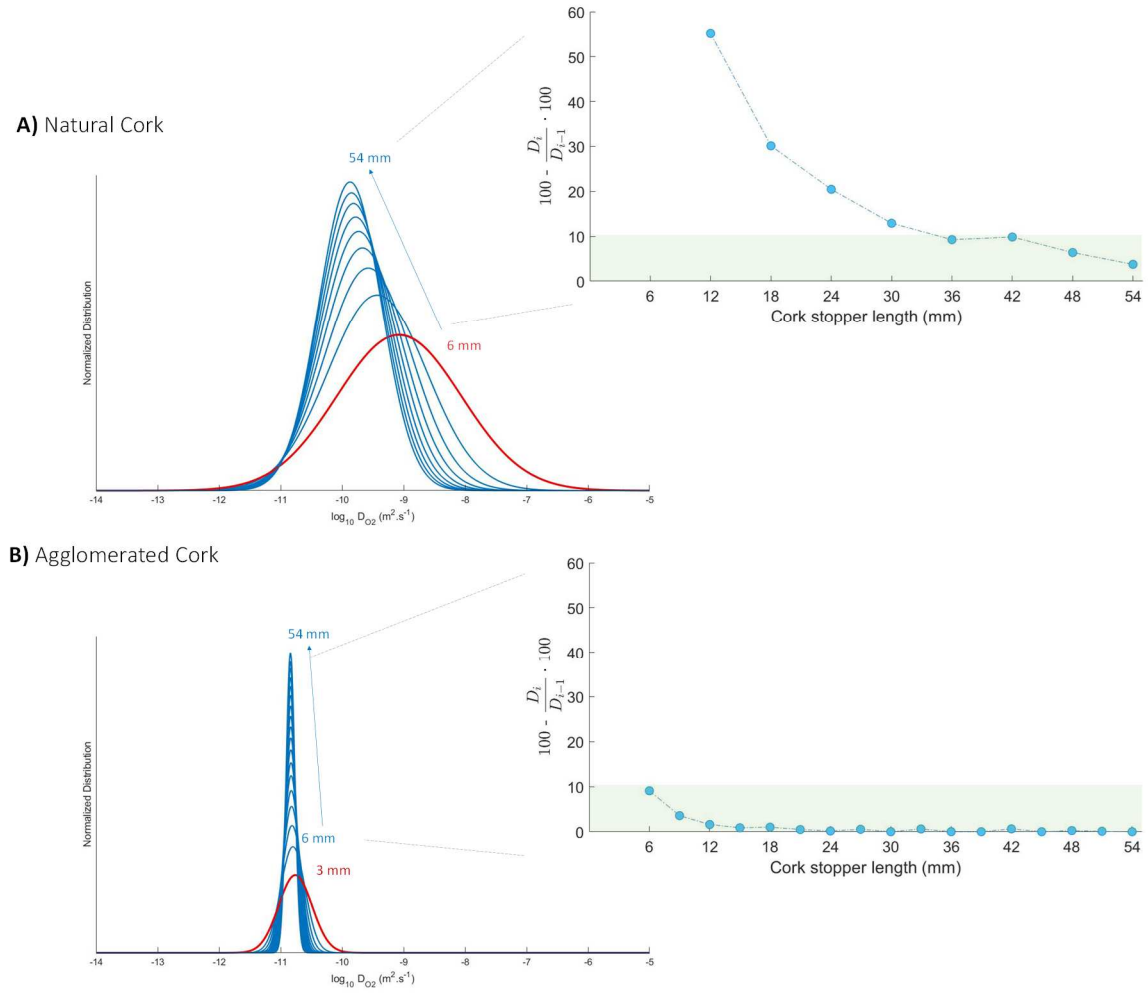

Figure 8: Distribution of the effective oxygen diffusion coefficients measured on 3 mm or 6 mm wafers, at 298 K (- red line), and extrapolation for stoppers having a length ranging from 6 mm to 54 mm with a step of 3 mm (- blue lines). A) Natural cork (n=15). B) Agglomerated cork (n=10).

Nevertheless, these results should be considered with great caution for any subsequent generalization to other types of stoppers for which experimentations should also be performed. The current objective was to assess the robustness of the extrapolation method for a stopper system having different degrees of heterogeneity. It should be noted that the experimental measurements of the effective oxygen diffusion coefficients and the extrapolations have been performed on a single quality of natural cork stopper and a single formulation of microagglomerated cork stopper. They are obviously not representative of all natural cork stoppers and agglomerated cork-based stoppers, respectively. In particular, the formulation of the agglomerated cork stopper and therefore the resulting cohesion depends strongly on the adhesive/cork ratio. Furthermore, only the transfer through the stopper is considered in this work, the interface being glued during the experiments. The oxygen transfer that can occur at the cork/glass interface can also have a strong impact on the effective diffusion coefficient[41].

5. Conclusion

We report a fast and simple method for determining the effective diffusion coefficient of oxygen through wine stoppers by performing permeation measurements using the manometric technique.

Firstly, the extrapolation model was validated by comparing the effective diffusion coefficients obtained on full-length stoppers with those extrapolated from permeation measurements on wafers for two different types of wine stoppers: natural cork and micro-agglomerated cork. The values of the effective diffusion coefficients obtained are similar with, in the case of natural cork, an experimental value of 19.0 x 10^{-11} $m^2.s^{-1}$ and an extrapolated value of 14.3 x 10^{-11} $m^2.s^{-1}$ and for samples of agglomerated cork, an experimental value of 1.8 x 10^{-11} $m^2.s^{-1}$ and an extrapolated value of 1.4 x 10^{-11} $m^2.s^{-1}$, respectively.

Secondly, oxygen transfer experiments were carried out on thin wafers of these two wine stoppers: natural cork, with its intrinsic heterogeneity due in particular to the presence of lenticels, and micro-agglomerated cork, which constitutes a more homogeneous system due to the polyurethane polymer network surrounding the cork particles. Performing measurements on thin wafers allowed to considerably reduce the analysis time (a few hours for a 3 mm thick wafer compared to one month for a whole stopper[33]). The intrinsic oxygen diffusion coefficients through a whole stopper were then determined using different calculation methods: arithmetic and harmonic means as well as an extrapolation method based on the statistical distribution of experimental data. This highlighted that this extrapolation method is always an appropriate means to determine the oxygen diffusion coefficient through wine stoppers. Particularly, in the case of natural cork stopper, it takes into account the local heterogeneities of the material. Nevertheless, for agglomerated cork stopper, the harmonic mean, which is simpler to calculate, gives a value close to that extrapolated, in accordance with a more homogeneous system. It can therefore be practically a good way of estimating, as a first approximation, the diffusion coefficient through a whole cork stopper from measurements performed on thin wafers.

Lastly, the effective length of the stopper above which the gain in resistance to oxygen transfer becomes insignificant, has been calculated both for natural and agglomerated stoppers (when considering only the transfer through the stopper). For natural cork, such calculation showed that the effective length is reached for a 36 mm length stopper. The effective length is reduced to only 6 mm in the case of agglomerated stopper. However, these results must be considered with caution for any extrapolation to oenological conditions as they are limited to the samples considered in this study and investigated under specific experimental conditions. This means a dry sample under vacuum, without partial pressure of water and ethanol vapors, without surface treatment of the stopper and without taking into account the possible transfer at the interface between the glass bottleneck and the wine stopper, each of these parameters deserving further studies.

Acknowledgments

We would like to thank Diam Bouchage as well as the French National Association of Research and Technology (ANRT) for their financial support and Julie Chanut's PhD grant (CIFRE n°2018/1273). The authors also thank Pr. Peter Krüger for his help in statistical analysis.

References

1. P. Lopes; C. Saucier; P.-L. Teissedre; Y. Glories, Impact of storage position on oxygen ingress through different closures into wine bottles. *Journal of Agricultural and Food Chemistry* **2006,** *54*, 6741-6746.
2. P. Lopes; M. A. Silva; A. Pons; T. Tominaga; V. Lavigne; C. Saucier; P. Darriet; M. Cabral; P.-L. Teissedre; D. Dubourdieu, Impact of the Oxygen Exposure during Bottling and Oxygen Barrier Properties of Different Closures on Wine Quality during Post-Bottling. In *Flavor Chemistry of Wine and Other Alcoholic Beverages*, American Chemical Society: 2012; Vol. 1104, pp 167-187.
3. P. Arapitsas; G. Speri; A. Angeli; D. Perenzoni; F. Mattivi, The influence of storage on the ''chemical age'' of red wines. *Metabolomics* **2014,** *10*, 816-832.
4. F. Venturi; C. Sanmartin; I. Taglieri; Y. Xiaoguo; G. Andrich; A. Zinnai, The influence of packaging on the sensorial evolution of white wine as a function of the operating conditions adopted during storage. *Agrochimica* **2016,** *60* (2), 150-159.
5. F. Venturi; C. Sanmartin; I. Taglieri; Y. Xiaoguo; M. F. Quartacci; C. Sgherri; G. Andrich; A. Zinnai, A kinetic approach to describe the time evolution of red wine as a function of packaging conditions adopted: Influence of closure and storage position. *Food Packaging and Shelf Life* **2017,** *13*, 44-48.
6. Opinion way Survey for Les professionnels du liège.**3-5 may 2017**
7. C. Roullier-Gall; D. Hemmler; M. Gonsior; Y. Li; M. Nikolantonaki; A. Aron; C. Coelho; R. D. Gougeon; P. Schmitt-Kopplin, Sulfites and the wine metabolome. *Food Chemistry* **2017,** *237*, 106-113.
8. Le bouchage des vins de Bourgogne (2) Ce qu'il faut savoir In *Bourgogne Amplitude 2015* B. I. d. V. d. Bourgogne, Ed. Beaune, 2015.
9. IPSOS survey for European Aluminium Foil.**2017**
10. E. J. Waters; Z. Peng; K. F. Pocock; P. J. Williams, The role of corks in oxidative spoilage of white wines. *Australian Journal of Grape and Wine Research* **1996**, 191-197.
11. T. Karbowiak; R. D. Gougeon; J.-B. Alinc; L. Brachais; F. Debeaufort; A. Voilley; D. Chassagne, Wine oxidation and the role of cork. *Critical Reviews in Food Science and Nutrition* **2010,** *50*, 20-52.
12. V. Oliveira; S. Knapic; H. Pereira, Classification modeling based on surface porosity for the grading of natural cork stoppers for quality wines. *Food and Bioproducts Processing* **2015,** *93*, 69-76.
13. ASTM D1434: Standard Test Method for Determining Gas Permeability Characteristics of Plastic Film and Sheeting; West Conshohocken, PA, U.S.A, 2015.
14. International Standard Organisation (ISO). ISO 15105-1:2007: Plastics - Film and sheeting - Determination of gas-transmission rate - Part 1 : differential-pressure method; Switzerland, 2007.
15. International Standard Organisation (ISO). ISO 15105-2:2003: Plastics - Film and sheeting - Determination of gas-transmission rate - Part 2 : equal-pressure method Switzerland, 2003.
16. K. Crouvisier-Urion; J.-P. Bellat; R. D. Gougeon; T. Karbowiak, Gas transfer through wine closures : A critical review. *Trends in Food Science & Technology* **2018,** *78*, 255-269.
17. P. Lopes; A. Silva; A. Pons; T. tominaga; V. Lavigne; C. Saucier; P. Darriet; P.-L. Teissedre; D. Dubourdieu, Impact of Oxygen Dissolved at Bottling and Transmitted through Closures on the Composition and Sensory Properties of a Sauvignon Blanc Wine during Bottle Storage. *Journal of Agricultural and Food Chemistry* **2009,** *57*, 10261-10270.
18. P. Lopes; C. Saucier; P.-L. Teissedre; Y. Glories, Main Routes of oxygen ingress through different closures into wine bottles. *Journal of Agricultural and Food Chemisty* **2007,** *55*, 5167-5170.
19. P. Lopes; C. Saucier; Y. Glories, Nondestructive Colorimetric Method To Determine the Oxygen Diffusion Rate through Closures Used in Winemaking. *Journal of Agricultural and Food Chemistry* **2005,** *53*, 6967-6973.
20. J. Ribéreau-Gayon, *Dissolution d'oxygène dans les vins. Contribution à l'étude des oxydations et des réductions dans les vins. Application à l'étude du vieillissement et des casses*. Delmas: Bordeaux, 1933.

21. L. Brotto; F. Battistutta; L. Tat; P. Comuzzo; R. Zironi, Modified nondestrcutive colorimetric method to evaluate the variability of oxygen diffusion rate through wine bottle closures. *Journal of Agricultural and Food Chemistry* **2010,** *58*, 3567-3572.
22. J.-C. Vidal; M. Moutonnet, Monitoring of oxygen in the gas and liquid phases of bottles of wine at bottling and during storage. *J. Int. Sci. Vigne Vin* **2006,** *40* (1), 35-45.
23. J.-C. Vidal; M. Moutounet, Impact des conditions opératoires au conditionnement et de la perméabilité du bouchon sur l'oxygène et l'évolution d'un vin blanc de sauvignon en bouteille. *Revue internet de viticulture et oenologie* **2011,** *3* (2), 1-16.
24. D. Bunner; A. Landrieux; M. Valade; E. Langleron; I. Tribaut-Sohier; D. Moncomble; L. Viaux; L. Bourdelet Walter; V. Chaperon; B. Gouez, La mesure de l'oxygène dans les bouteilles par chimiluminescence. *Vigneron Champenois* **2010,** *131* (1), 84-101.
25. J. B. Dieval; J.-C. Vidal; O. Aagaard, Measurement of the oxygen transmission rate of co-extruded wine bottle closures using a luminescence-based technique. *Packaging technology and Science* **2011,** *24*, 375-385.
26. ASTM F1927: Standard Test Method for Determination of Oxygen Gas Transmission Rate, Permeability and Permeance at Controlled Relative Humidity Through Barrier Materials Using a Coulometric Detector; West Conshohocken, PA, U.S.A, 2014.
27. B. C. Rankine; K. F. Pocock, Alkalimetric determination of sulphur dioxide in wine. *Aust. Wine Brew. Spirit Rev.* **1970,** *88* (8), 40-44.
28. M. Ripper, Die Schweflige säure im wiene und duren bestimmung. *Journal für Praktische Chemie* **1892,** *46*, 482-473.
29. D. Rabiot; J. Sanchez; J. M. Aracil, Study of the oxygen transfer through synthetic corks for wine conservation. In *Second Europeen congress of chemical engineering*, Montpellier, France, 1999.
30. J. Sanchez; J. M. Aracil, Perméabilité gazeuse de différents obturateurs. *Bulletin de l'OIV* **1998,** *71*, 279-283.
31. C. Brazinha; A. P.Fonseca; H. Pereira; O. M.N.D.Teodoro; J. G.Crespo, Gas transport through cork: Modelling gas permeation based on the morphology of a natural polymer material. *Journal of Membrane Science* **2013,** *428*, 52-62.
32. D. P. Faria; A. L. Fonseca; H. Pereira; O. M. N. D. Teodoro, Permeability of Cork to Gases. *Journal of Agricultural and Food Chemistry* **2011,** *59*, 3590-3597.
33. S. Lequin; D. Chassagne; T. Karbowiak; J.-M. Simon; C. Paulin; J.-P. Bellat, Diffusion of oxygen in cork. *Journal of Agricultural and Food Chemistry* **2012,** *60*, 3348-3356.
34. A. Lagorce-Tachon; T. Karbowiak; C. Paulin; J.-M. Simon; R. D. Gougeon; J.-P. Bellat, About the role of the bottleneck/cork interface on oxygen transfer. *Journal of Agricultural and Food Chemistry* **2016,** *64* (35), 6672-6675.
35. A. Lagorce-Tachon; T. Karbowiak; J.-M. Simon; R. D. Gougeon; J.-P. Bellat, Diffusion of oxygen through cork stopper: Is it a Knudsen or a Fickian mechanism? *Journal of Agricultural and Food Chemistry* **2014,** *62* (37), 9180-9185.
36. T. Karbowiak; K. Crouvisier-Urion; A. Lagorce; J. Ballester; A. Geoffroy; C. Roullier-Gall; J. Chanut; R. D. Gougeon; P. Schmitt-Kopplin; J.-P. Bellat, Wine aging: a bottleneck story. *Npj Science of Food* **2019,** *14*.
37. K. S. W. Sing, Reporting physisorption data for gas/solid systems with special reference to the determination of surface area and porosity (Recommendations 1984). *Pure and Applied Chemistry* **1985,** *57* (4), 603.
38. G. T. Brower; G. Thodos, Vapor pressures of liquid oxygen between the triple point and critical point. *Journal of Chemical & Engineering Data* **1968,** *13* (2), 262-264.
39. K. Crouvisier-Urion; J. Chanut; A. Lagorce; P. winckler; Z. Wang; P. Verboven; B. Nicolai; J. Lherminier; E. Ferret; R. Gougeon; J.-P. Bellat; T. Karbowiak, Four hundred years of cork imaging: New advances in the characterization of the cork structure. *Scientific Reports* **2019**.
40. A. B. Marin; E. M. Jorgensen; J. A. Kennedy; J. Ferrier, Effects of Bottle Closure Type on Consumer Perceptions of Wine Quality. *American Journal of Enology and Viticulture* **2007,** *58* (2), 182.

41. J. Chanut; J.-P. Bellat; R. D. Gougeon; T. Karbowiak, Controlled diffusion by thin layer coating: The intricate case of the glass-stopper interface. *Food Control* **2021,** *120*, 107446.